THE JOURNAL OF BIOLOGICAL CHEMISTRY VOL. 286, NO. 26, pp. 23388–23396, July 1, 2011

Chromatin-modifying Complex Component Nurf55/p55 Associates with Histones H3 and H4 and Polycomb Repressive Complex 2 Subunit Su(z)12 through Partially Overlapping Binding Sites[S]

Received for publication, November 29, 2010, and in revised form, April 27, 2011 Published, JBC Papers in Press, May 5, 2011, DOI 10.1074/jbc.M110.207407

Agnieszka J. Nowak[‡1], Claudio Alfieri[‡1], Christian U. Stirnimann[‡2], Vladimir Rybin[‡], Florence Baudin[‡§], Nga Ly-Hartig[‡], Doris Lindner[‡], and Christoph W. Müller[‡3]

From the [‡]European Molecular Biology Laboratory, 69117 Heidelberg, Germany and [§]UJF-EMBL-CNRS UMI 3265, Unit of Virus Host-Cell Interactions, 38042 Grenoble Cedex 9, France

Drosophila **Nurf55 is a component of different chromatin-modifying complexes, including the PRC2 (Polycomb repressive complex 2). Based on the 1.75-Å crystal structure of Nurf55 bound to histone H4 helix 1, we analyzed interactions of Nurf55 (Nurf55 or p55 in fly and RbAp48/46 in human) with the N-terminal tail of histone H3, the first helix of histone H4, and an N-terminal fragment of the PRC2 subunit Su(z)12 using isothermal calorimetry and pulldown experiments. Site-directed mutagenesis identified the binding site of histone H3 at the top of the Nurf55 WD40 propeller. Unmodified or K9me3- or K27me3-containing H3 peptides were bound with similar affinities, whereas the affinity for K4me3-containing H3 peptides was reduced. Helix 1 of histone H4 and Su(z)12 bound to the edge of the β-propeller using overlapping binding sites. Our results show similarities in the recognition of histone H4 and Su(z)12 and identify Nurf55 as a versatile interactor that simultaneously contacts multiple partners.**

Polycomb group proteins play important roles in maintaining the silenced state of homeotic genes, as well as in other biological processes, including X chromosome inactivation, germ line development, stem cell pluripotency, and cancer metastasis (reviewed in Refs. 1 and 2). Thus far, three different major Polycomb repressive complexes have been identified in *Drosophila melanogaster*: PRC1, PRC2, and PhoRC (Pleiohomeotic-repressive complex).

Drosophila PRC1 contains four core subunits, including the chromodomain protein Polycomb, which specifically binds the trimethylated Lys-27 of the histone H3 tail. *In vitro*, high concentrations of PRC1 establish a compact higher order chromatin structure that inhibits ATP-dependent chromatin remodeling and transcription of Polycomb group target genes (3). PRC2 is phylogenetically the most ancient of the Polycomb repressive complexes (2) and forms the functional core of the Polycomb group repression machinery. It consists of the four subunits E(z) (Enhancer of zeste), Su(z)12 (Suppressor of zeste 12), Esc (Extra sex combs), and Nurf55 (4–7). Histone methyltransferase activity is associated with the SET domain of E(z), which specifically methylates Lys-27 in histone H3 (H3K27). The third Polycomb repressive complex, PhoRC, contains the sequence-specific DNA-binding protein Pleiohomeotic, homologous to the mammalian transcription factor YY1, and the MBT (malignant brain tumor) domain protein dSfmbt, which binds mono- and dimethylated lysines of histone H3 and H4 tails (8).

Nurf55 is a non-catalytic subunit of PRC2 that is necessary *in vitro* to ensure high-affinity binding of the complex to nucleosomes (7, 9). Nurf55 is also found in several other chromatin-modifying complexes, including HAT1 (histone acetyltransferase 1) and histone deacetylase complexes, CAF-1 (chromatin assembly factor-1), and the ATP-dependent nucleosome-remodeling complexes NURF and NuRD (reviewed in Ref. 10). In addition, Nurf55 forms complexes with histones H3 and H4 and with the essential centromeric variant CenH3 (11). Nurf55 was proposed to act as a recruiting factor that tethers different complexes to their substrate nucleosomes, as well as a histone chaperone that deposits H3/H4 dimers during replication-dependent and replication-independent nucleosome assembly (12). The x-ray structure of *Drosophila* Nurf55 has recently been determined alone and in complex with a fragment of histone H4 at 2.9 and 3.2 Å, respectively (13). In addition, the structure of the human ortholog RbAp46 bound to a histone H4 peptide has been reported at 2.4-Å resolution (14). Nurf55 forms a seven-bladed β-propeller characteristic for the WD40 family of proteins, known to be involved in protein-protein interactions (15). The β-propeller is preceded by a long N-terminal helix.

On the basis of our high-resolution (1.75 Å) structure of Nurf55 bound to the first helix of histone H4, we analyzed the interactions of Nurf55 with histones H3 and H4 and the PRC2 component Su(z)12. We identified a cluster of highly conserved negatively charged residues at the top surface of the Nurf55 β-propeller that mediates the binding of the N-terminal tail of histone H3. We show that the binding pocket at the edge of the Nurf55 β-propeller that binds the first helix of histone H4 is also involved in the interaction with Su(z)12.

[S] The on-line version of this article (available at http://www.jbc.org) contains supplemental "Experimental Procedures," Figs. S1–S3, and Table 1.

The atomic coordinates and structure factors (code 2XYI) have been deposited in the Protein Data Bank, Research Collaboratory for Structural Bioinformatics, Rutgers University, New Brunswick, NJ (http://www.rcsb.org/).

[1] Both authors contributed equally to this work.

[2] Supported by Marie Curie Framework Program 7 and the European Molecular Biology Organization Long-Term Fellowship Program.

[3] To whom correspondence should be addressed: European Molecular Biology Laboratory, Meyerhofstr. 1, 69117 Heidelberg, Germany. Fax: 49-6221-387-519; E-mail: cmueller@embl.de.

EXPERIMENTAL PROCEDURES

Protein Expression and Purification—Wild-type and mutant *Drosophila* Nurf55 (p55) proteins were expressed in Sf21 cells as N-terminal, tobacco etch virus-cleavable, His-tagged fusion proteins and purified using standard procedures as described under supplemental "Experimental Procedures." The CD spectra of wild-type and mutant Nurf55 proteins confirmed that the overall structure was preserved in all mutants (supplemental Fig. S1). FLAG-tagged Su(z)12 and E(z) proteins were expressed separately or coexpressed with wild-type and mutant Nurf55 proteins in Sf21 insect cells and purified using anti-FLAG affinity resin as described (9). Su(z)12 fragments were expressed as tobacco etch virus-cleavable GST fusion proteins in *Escherichia coli* and purified using standard procedures (see supplemental "Experimental Procedures"). For the binding experiments, histone H3/H4 heterodimers, $H4_{26-45}$ peptide, and lysozyme (Sigma) were cross-linked to Dynabeads (Dynal Biotech) according to the manufacturer's instructions.

Crystallographic Structure Determination—For crystallization, purified Nurf55 was mixed with the $H4_{26-45}$ peptide at a ratio of 1:3. The best crystals were obtained by mixing 1 μl of complex and 1 μl of precipitant solution (35% (v/v) PEG 400 and 100 mM MES, pH 6) using the hanging drop vapor diffusion method. Diffraction data were collected at beamline ID23-2 at the European Synchrotron Radiation Facility (Grenoble, France) and were processed and scaled using the programs XDS and XSCALE (16). The crystals diffracted to 1.7 Å and belonged to space group $P2_1$, with one molecule/asymmetric unit. The structure of Nurf55 bound to the H4 peptide was solved by molecular replacement using the program PHASER v1.3 (17) with the structure of Nurf55 alone (Protein Data Bank code 3C99, chain A) (13) as a search model. The model was rebuilt with the program Coot v0.4 (18) and refined using the program Phenix v1.3 (19) to an *R*-factor of 17.3% and a free *R*-factor of 20.5% (supplemental Table 1).

Isothermal Titration Calorimetry (ITC)[4] *Measurements*—ITC measurements were performed at 25 °C using a MicroCal VP-ITC calorimeter. All proteins were dialyzed overnight against ITC buffer (10 mM Tris-HCl, pH 7.5, 150 mM NaCl, and 1 mM β-mercaptoethanol). Lyophilized peptides were resuspended in ITC buffer. Each titration experiment consisted of injecting 10 μl of a 200 μM peptide solution into 2 ml of a 10 μM protein solution at time intervals of ~5 min. Experiments in which the K_D was higher than 10 μM were repeated with 2.5 times higher concentrations of protein and peptide. For competition ITC experiments, we used 8–12 μM Nurf55 preincubated in the cell with 30–100 μM competitor peptide (see Table 2). To fit an apparent dissociation constant ($K_{D(app)}$), we used standard procedures (20) implemented in the MicroCal Origin 7.0 software package.

RESULTS AND DISCUSSION

Binding of Nurf55 to Histone H4—Nurf55 from *D. melanogaster* and its two human homologs, RbAp46 and RbAp48, have been reported to bind the first helix of histone H4 (21, 22). Using ITC, we found that full-length recombinant Nurf55 specifically bound to a 20-residue peptide corresponding to the first helix of H4 (hereafter referred to as the H4 peptide) with high affinity (K_D = 35 nM) (Table 1). In contrast, the histone tail peptide $H4_{1-15}$ and a scrambled $H4_{26-45}$ peptide with the same amino acid composition but different primary sequence did not bind to Nurf55. Nurf55 was co-crystallized with this peptide, and the structure was solved by molecular replacement at 1.75-Å resolution using the structure of *Drosophila* Nurf55 without peptide as a search model (13).

The high resolution of the Nurf55-H4 peptide complex structure (Figs. 1 and 2) allows for a more detailed analysis of the interactions between Nurf55 and the H4 peptide than previously possible. The Nurf55 binding surface consists of a hydrophobic moiety formed by the N-terminal helix and residues from blade 6 and a negatively charged moiety formed mainly by residues protruding from the short helix in the loop connecting two strands in blade 6 (Figs. 1*A* and 2). Most importantly, Arg-39 of the H4 peptide (H4R39) (Fig. 2*A*) forms a network of hydrogen bonds involving two main chain carbonyl groups of Nurf55 (Asp-362 and Gly-366), the side chain of Gln-358, and a water-mediated hydrogen bond with Asp-365 (Fig. 2). Mutating H4R39 to alanine caused a 3000-fold decrease in the binding affinity for Nurf55 (K_D = 115 μM). Similarly, mutating Gln-358 of Nurf55 to alanine resulted in a >500-fold decrease in the affinity for H4 (K_D = 26 μM). Two other arginine residues in the H4 peptide, H4R36 and H4R40, also play important roles in Nurf55 binding. H4R36 forms two hydrogen bonds with Asp-362 of Nurf55, and H4R40 forms one direct and one water-mediated hydrogen bond with Asp-365. Mutating these two arginines to alanine lowered the affinity for Nurf55 by ~20-fold (K_D = 0.87 μM). In contrast, mutating both arginines to lysine only led to ~3-fold weaker binding to Nurf55 (K_D = 0.11 μM), indicating that the positively charged surface of the H4 helix rather than the two arginines is important for binding to Nurf55 (Table 1).

Two aspartate residues of Nurf55 (Asp-362 and Asp-365) that form hydrogen bonds with H4R36, H4R39, and H4R40 (see above) contribute to the negative surface charge on one side of the Nurf55 binding pocket (Figs. 1*B*, 2, and 3*A*). Mutating both residues to alanine strongly lowered the binding affinity for the H4 peptide (K_D = 9.6 μM), whereas mutating them to glutamate, preserving the negative surface charge of the binding pocket, had a much weaker effect (K_D = 0.44 μM). To test the contribution of hydrophobic residues to the Nurf55-H4 interaction, Leu-35, Phe-372, and Ile-373 of Nurf55 were mutated to serine (Fig. 3*A*). The Nurf55 triple mutant L35S/F372S/I373S bound the H4 peptide with significantly lower affinity (K_D = 15.4 μM).

Interaction of Nurf55 with the N-terminal Tail of Histone H3—Binding of Nurf55 to histone H3 and H4 and to an *in vitro* reconstituted complex of H3/H4 dimers and tetramers in dynamic equilibrium has been reported (13). Many of the known interactions between histones and other proteins are mediated by N-terminal histone tails, which are poorly structured and accessible for binding in the context of the H3/H4 dimer and the nucleosome. We therefore tested binding of Nurf55 to a 28-residue H3 tail peptide ($H3_{1-28}$) using ITC (Fig.

[4] The abbreviation used is: ITC, isothermal titration calorimetry.

TABLE 1
Binding affinities of wild-type and mutant Nurf55 for H4 and H3 peptides and Su(z)12-1

$H4_{26-45}$: IQGITKPAIRR$_{36}$LAR$_{39}$R$_{40}$GGVKR						
Protein	***Peptide*** [a]	***K_D (μM)*** [b]	***N***	***ΔG° (kcal/mol)***	***ΔH° (kcal/mol)***	***TΔS° (kcal/mol)***
Wt Nurf55	$H4_{26-45}$	0.035±0.001	1.01	-10.3	-18.9	-8.6
	H4-R39A	115±8	1.00	-5.4	-18.5	-13.1
	H4-R36A,R40A	0.87±0.04	0.97	-8.3	-14.8	-6.5
	H4-R36K,R40K	0.11±0.01	0.97	-9.5	-15.5	-6.0
	$H4_{26-45}$ *(scrambled)* [c]	> 500	-	-	-	-
	$H4_{1-15}$ [c]	> 500	-	-	-	-
	$H4_{1-15}$ *(scrambled)* [c]	> 500	-	-	-	-
Mutant - H4/Su(z)12 site						
N31A	$H4_{26-45}$	0.057±0.004	0.93	-9.9	-22.2	-12.3
N31D	$H4_{26-45}$	0.34±0.01	1.00	-8.8	-19.6	-10.7
D362A/D365A	$H4_{26-45}$	9.6±0.8	0.96	-6.9	-19.0	-12.2
D362E/D365E	$H4_{26-45}$	0.44±0.03	1.06	-8.7	-9.5	-0.9
D362N/D365N	$H4_{26-45}$	1.3±0.1	1.03	-8.0	-20.3	-12.2
Q358A	$H4_{26-45}$	26±2	1.00	-6.3	-17.3	-11.0
L35S/F372S/I373S	$H4_{26-45}$	15.4±1.4	1.00	-6.6	-15.0	-8.4
Mutant - H3 site						
D322N/E323K	$H4_{26-45}$	0.040±0.003	1.00	-1.0	-16.0	-5.9
E235Q/D252K/E279Q	$H4_{26-45}$	0.034±0.004	0.99	-10.2	-15.7	-5.5
$H3_{1-28}$: ARTK$_4$QTARK$_9$STGGKAPRKQLATKAARK$_{27}$S						
Protein	***Peptide*** [a]	***K_D (μM)*** [b]	***N***	***ΔG° (kcal/mol)***	***ΔH° (kcal/mol)***	***TΔS° (kcal/mol)***
Wt Nurf55	$H3_{1-28}$	1.6±0.1	1.11	-7.9	-14.5	-6.6
	$H3_{1-28}$K4me3	6.4±0.6	0.83	-7.1	-18.0	-10.9
	$H3_{1-28}$K9me3	1.22±0.06	1.19	-8.1	-15.8	-7.7
	$H3_{1-28}$K27me3	0.69±0.05	1.11	-8.4	-15.0	-6.5
	$H3_{1-28}$ *(scrambled)* [c]	> 500	-	-	-	-
	$H3_{1-15}$	2.1±0.05	1.00	-7.8	-18.4	-10.6
	$H3_{1-15}$K4me3	> 500	-	-	-	-
	$H3_{1-15}$K9me3	22±1	1.00	-6.3	-12.4	-6.05
	$H3_{1-15}$ *(scrambled)* [c]	> 500	-	-	-	-
	$H3_{13-28}$	18±1	1.00	-6.5	-14.0	-7.5
	$H3_{6-20}$	> 500	-	-	-	-
Mutant - H4/Su(z)12 site						
D362A/D365A	$H3_{1-28}$	1.4±0.2	1.13	-8.0	-23.8	-15.8
L35S/F372S/I373S	$H3_{1-28}$	1.8±0.1	1.06	-7.9	-24.5	-16.6
Mutant – H3 site						
D322N/E323K	$H3_{1-28}$	17.4±1.8	1.16	-6.5	-14.7	-8.2
	$H3_{1-15}$	8.8±1.4	0.88	-6.9	-13.6	-6.7
E235Q/D252K/E279Q	$H3_{1-28}$	> 500	-	-	-	-
	$H3_{1-15}$	> 500	-	-	-	-
E235Q/D252K/E279Q/ D322N/E323K	$H3_{1-28}$	> 500	-	-	-	-
Su(z)12-1 construct						
Protein	***Peptide*** [a]	***K_D (μM)*** [b]	***N***	***ΔG° (kcal/mol)***	***ΔH° (kcal/mol)***	***TΔS° (kcal/mol)***
Wt Nurf55	Su(z)12-1[a]	24±1	1.00	-6.3	-21.9	-15.6
Mutant - H4/Su(z)12 site						
D362A/D365A	Su(z)12-1	> 500	-	-	-	-
L35S/F372S/I373S	Su(z)12-1	> 500	-	-	-	-

[a] H3 and H4 peptides were chemically synthesized. Construct Su(z)12-1 comprises *Drosophila* Su(z)12 residues 1–100 as shown in Fig. 5*A* and was expressed and purified as described under "Experimental Procedures."
[b] Errors of the K_D are fitting errors using the data evaluation program.
[c] The following peptides were used as internal controls: $H4_{26-45(scrambled)}$, PKGIRTAARGRGQVRIIRLK; $H4_{1-15}$, TGRGKGGKGLGKGGA; $H4_{1-15(scrambled)}$, KGKGGAK-GRGGLGGT; $H3_{1-28(scrambled)}$, QTALTSRTGRRTKSQAAAKPKGKAAKRK; and $H3_{1-15(scrambled)}$, TRSTAAQTKGGRKAK.

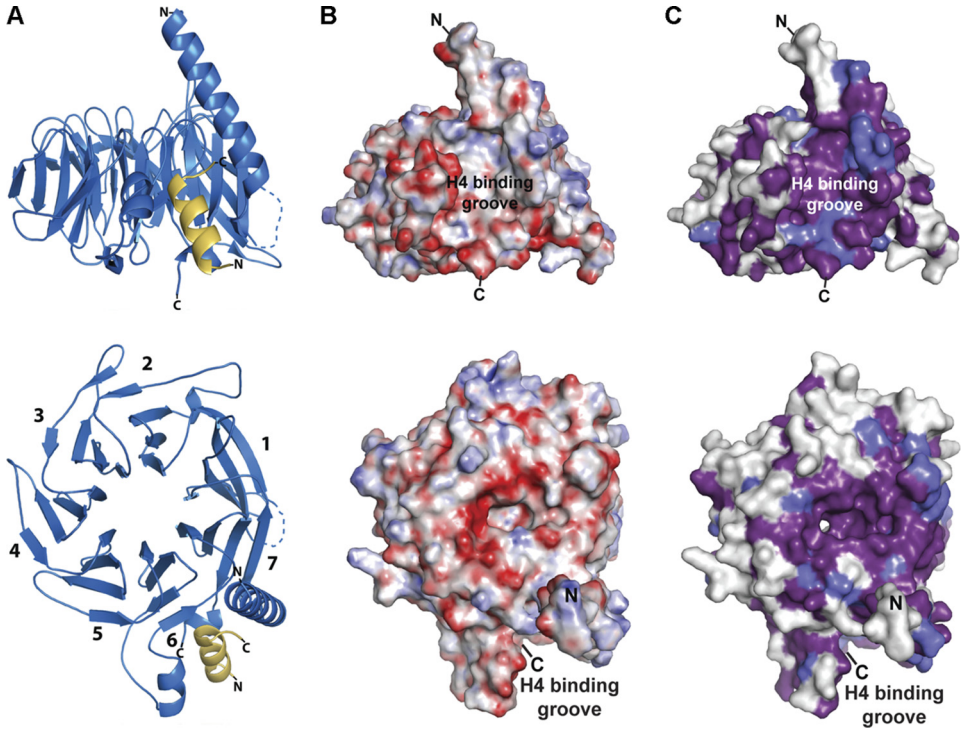

FIGURE 1. **Overview of the Nurf55-H4 peptide structure.** *A*, front and top views (turned by 90° around a horizontal axis) of the Nurf55-H4 peptide structure. Nurf55 is depicted in *marine*, and the H4 peptide is shown in *yellow*. *Numbers* in the *lower left panel* indicate the blades of the β-propeller. *B*, electrostatic potential mapped on the surface of Nurf55. Acidic patches are shown in *red*, neutral patches in *white*, and basic patches in *blue* (overall range from −30 to +30 *kT*). *C*, sequence conservation mapped on the surface of Nurf55. Completely conserved residues are indicated in *violet*, residues >80% conserved in *purple*, and residues >60% conserved in *light blue*.

3*A*) and found that Nurf55 bound this peptide with low but significant affinity ($K_D = 2\ \mu M$) (Table 1). The shorter peptide $H3_{1-15}$ was bound with the same affinity as the longer peptide $H3_{1-28}$. In contrast, peptide $H3_{13-28}$ was bound with 9-fold reduced affinity, whereas peptide $H3_{6-20}$ did not bind. Scrambled $H3_{1-15}$ and $H3_{1-28}$ peptides also did not bind Nurf55, further confirming the specificity of the observed interaction (Table 1). Competition experiments showed that peptide $H3_{1-15}$ could still bind Nurf55 even when peptide $H3_{13-28}$ was present in excess, whereas in the reverse experiment, the second peptide did not bind Nurf55 (Table 2). We therefore conclude that peptide $H3_{1-15}$ is the stronger interactor and preferentially occupies the H3-binding site in Nurf55, although peptide $H3_{13-28}$ maintains some binding capacity.

Trimethylation of Lys-4 (K4me3) in peptide $H3_{1-15}$ strongly reduced binding to Nurf55 ($K_D > 500\ \mu M$), whereas the effect was smaller for K9me3 ($K_D = 22\ \mu M$). In the context of the longer $H3_{1-28}$ peptide, the binding affinity for the K4me3-containing peptide was reduced by a factor of 3, whereas longer K9me3- or K27me3-containing H3 peptides bound with similar affinities as the unmodified peptide (Table 1). At present, it is unclear why the K9me3- or K27me3-containing $H3_{1-28}$ peptides bound with similar affinities as the unmodified H3 peptides and better than the shorter K9me3-containing $H3_{1-15}$ peptide (Table 1). We speculate that trimethylation of Lys-9 and Lys-27 favors a slightly different conformation of the $H3_{1-28}$ peptide that allows the additional C-terminal residues to contribute to the binding (Table 1). Trimethylation of Lys-4 in histone H3 is generally associated with active chromatin, and trimethylation of Lys-9 and Lys-27 with repressive chromatin. The capacity of Nurf55 to bind unmethylated and "repressive" K9me3- and K27me3-containing histone H3 peptides equally well, but also "active" K4me3-containing peptides (although with reduced affinity), might reflect its versatile roles in different chromatin-modifying complexes.

Sequence conservation mapped on the surface of Nurf55 revealed a patch of highly conserved residues, many of them negatively charged, on the top of the β-propeller surrounding the central channel (Fig. 1, *B* and *C*). This site is commonly used for peptide binding in WD40 proteins (15) and could conceivably serve as the interaction surface for the positively charged H3 tail. To test this hypothesis, double, triple, and 5-fold mutations were introduced in Nurf55, changing conserved acidic residues in this region into uncharged or basic residues (Fig. 3*C*). The CD spectra confirmed that the overall structure of the mutants was preserved (supplemental Fig. S1). The mutant proteins were tested for histone H3 binding using ITC. Although one mutant (D322N/E323K) bound peptide $H3_{1-28}$ with 11-fold reduced affinity, the two other mutants (E235Q/D252K/E279Q and E235Q/D252K/E279Q/D322N/E323K) no longer showed binding to the H3 peptide, confirming that we correctly identified the interaction site (Table 1). Mutations in the H4-binding pocket (D362A/D365A and L35S/F372S/I373S) that interfered with H4 binding did not change the affinity for the H3 tail. Similarly, mutations in the H3-binding pocket (D322N/E323K and E235Q/D252K/E279Q) did not affect the affinity for the H4 peptide (Table 1). Competition experiments also showed that the H3 peptide bound to Nurf55 with similar affinity in the presence of an excess of the H4 peptide and that H4 binding was similarly not affected by an excess

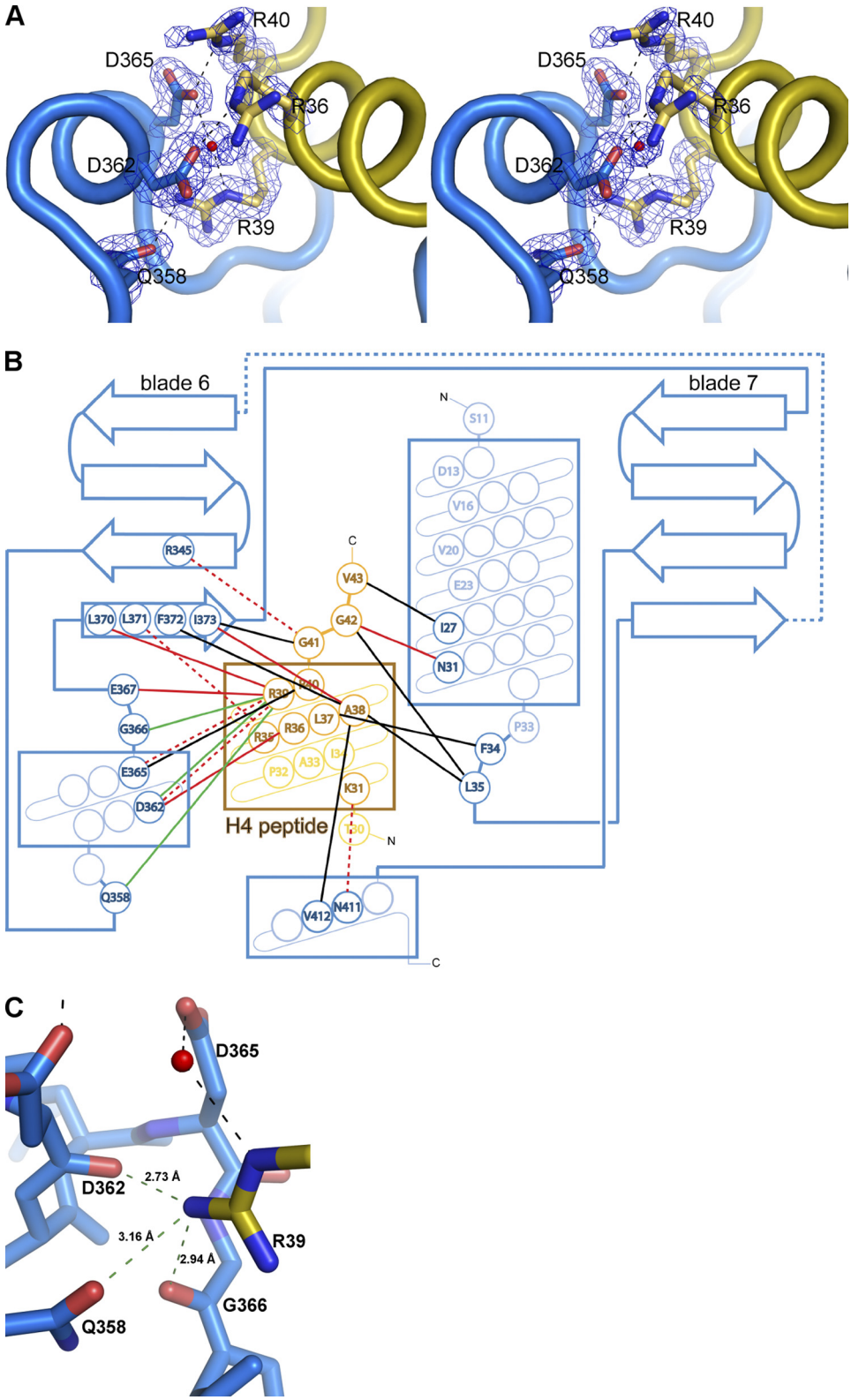

FIGURE 2. **Overview of the Nurf55-peptide interaction.** *A*, stereo view of polar interactions between Nurf55 and the H4 peptide. Nurf55 and the peptide are depicted as *blue* and *yellow ribbons*, respectively. Interacting residues enclosed by a $2F_o - F_c$ electron density map at 1.0σ are depicted in *stick* representation. *B*, schematic representation of the Nurf55-peptide interactions. The three helices and blade 6 forming the binding pocket and blade 7 are depicted in *blue*, the connecting residues between blades 7 and 6 as a *dashed blue line*, and the H4 peptide in *orange*. Hydrophobic interactions are drawn in *black*, hydrogen bonds in *red*, and water-mediated hydrogen bonds as *dashed red lines*. The hydrogen bond network shown in *C* is indicated with *green lines*. *C*, close-up view of the hydrogen bond network between the NH_2 group of Arg-39, the carboxamide of Gln-358, and the main chain carbonyls of Asp-362 and Gly-366. The network is indicated with *dashed green lines*.

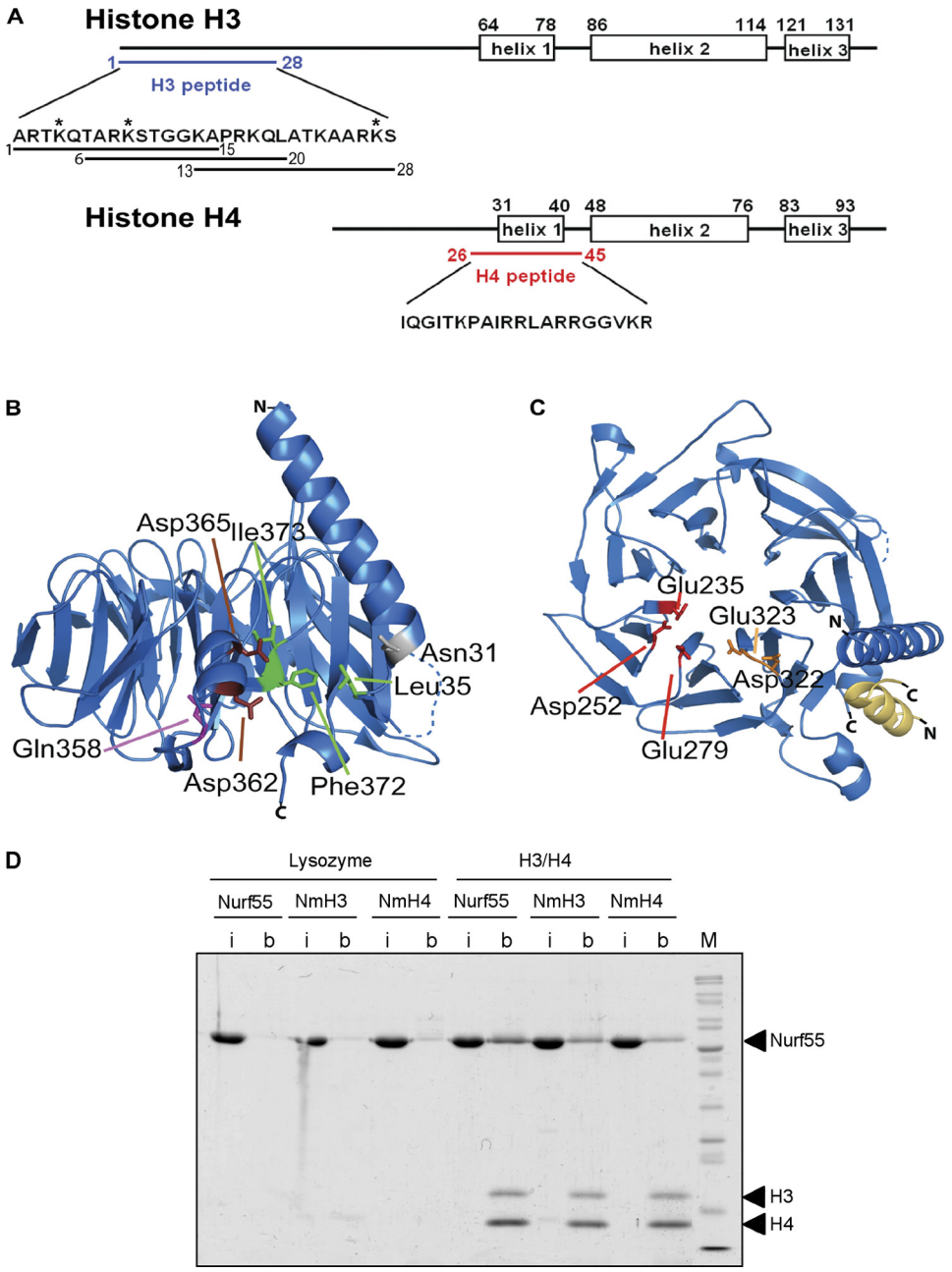

FIGURE 3. **Interaction of Nurf55 with histones H3 and H4.** *A*, secondary structure elements of histones H3 and H4 from *D. melanogaster*. Peptides $H3_{1-28}$, $H3_{1-15}$, $H3_{6-20}$, $H3_{13-28}$, and $H4_{26-45}$ used for ITC measurements and pulldown assays are indicated. Peptides containing trimethylated Lys-4, Lys-9, and Lys-27 residues as indicated by *asterisks* were tested for Nurf55 binding. The sequences of both peptides are given. *B*, side view of the Nurf55 β-propeller. Residues mutated in the H4-binding groove are depicted. *C*, top view of Nurf55 with the residues mutated in the H3 tail-binding site indicated. *D*, site-directed Nurf55 mutants of the H3-binding site (E235Q/D252K/E279Q; *NmH3*) and the H4-binding site (D362A/D365A; *NmH4*). Wild-type Nurf55 or Nurf55 mutants E235Q/D252K/E279Q and D362A/D365A were pulled down by histone H3/H4 dimers cross-linked to Dynabeads. Lysozyme was also cross-linked to beads and was used as a negative control. In each experiment, the input lane (*i*) contains one-tenth of the protein used in each of the pulldown assays, and *lane b* corresponds to the proteins pulled down. *Lane M*, molecular mass markers.

of the H3 peptide (Table 2). Nurf55 therefore uses two independent binding sites for interactions with the H3 tail and H4 helix 1.

Binding of the H3/H4 Heterodimer to Nurf55—The mechanism by which Nurf55 binds histones H3 and H4 is poorly understood. H4 helix 1 is not accessible for binding Nurf55 in the conformation that it adopts in nucleosomes (23), in H3/H4 dimers or tetramers, or in H3/H4 dimers bound to the histone chaperone Asf1 (24, 25). Therefore, the H3/H4 dimer must undergo a structural rearrangement upon binding to Nurf55 making helix 1 of histone H4 accessible for interaction (13). How Nurf55 initially recruits the H3/H4 dimer is also unclear.

Pulldown experiments using site-directed Nurf55 mutants of the H3-binding site (E235Q/D252K/E279Q) or the H4-binding site (D362A/D365A) with significantly lower affinities for the respective peptides (Table 1) showed reduced but not completely abolished binding to H3/H4 dimers (Fig. 3*D*), in agreement with the existence of two independent binding sites. The H4-binding site mutant bound weaker to the H3/H4 dimer compared with the H3-binding site mutant (Fig. 3*D*), consistent

TABLE 2
Competitive binding of the H3 and H4 peptides and the Su(z)12-1 construct

Competition experiment	Nurf55	Peptide with fixed concentration	Concentration	Peptide with variable concentration	$K_{D(app)}$ [a]
	μM		μM		μM
$H3_{13-28}$ + $H3_{1-15}$	8.8	$H3_{13-28}$	33	$H3_{1-15}$	4.5 ± 0.3
$H3_{1-15}$ + $H3_{13-28}$	8.8	$H3_{1-15}$	33	$H3_{13-28}$	> 250
$H4_{26-45}$ + $H3_{1-28}$	8.3	$H4_{26-45}$	68	$H3_{1-28}$	0.98 ± 0.04
$H3_{1-28}$ + $H4_{26-45}$	8.3	$H3_{1-28}$	66	$H4_{26-45}$	0.09 ± 0.01
$H3_{1-28}$ + Su(z)12-1	7.8	$H3_{1-28}$	95	Su(z)12-1	33 ± 4
Su(z)12-1 + $H3_{1-28}$	11.6	Su(z)12-1	100	$H3_{1-28}$	2.21 ± 0.25
$H4_{26-45}$ + Su(z)12-1	7.9	$H4_{26-45}$	95	Su(z)12-1	110 ± 3
Su(z)12-1 + $H4_{26-45}$	11.6	Su(z)12-1	100	$H4_{26-45}$	ND[b]

[a] Errors of the $K_{D(app)}$ are fitting errors using the data evaluation program.
[b] ND, no K_D could be determined presumably because of precipitation of Nurf55.

with the higher affinity of the H4 peptide compared with the H3 peptide for Nurf55 (Table 1).

The presence of two independent Nurf55 binding sites for the H3 N-terminal tail and for H4 helix 1 argues against a sequential binding mechanism. Nevertheless, H3 tail binding is presumably the more rapid initial targeting step, bringing Nurf55 in proximity to the H3/H4 dimers or tetramers, whereas H4 peptide binding is probably slower, as it requires a conformational change that makes helix 1 of histone H4 accessible for binding into the groove at the side of the β-propeller (Fig. 3*B*). Helix 1 of histone H4 is located opposite to the interface of the H3/H4 dimer, with the second dimer in the H3/H4 tetramer. Binding of Nurf55 to this helix would therefore not interfere with the formation of H3/H4 tetramers. The *in vitro* reconstituted Nurf55-H3/H4 complex migrated predominantly like a complex of ~70 kDa in size exclusion chromatography that would correspond to one molecule of Nurf55 bound to one H3/H4 dimer (75.3 kDa) (supplemental Fig. S2*A*). Analytical ultracentrifugation also showed the presence of a 75-kDa complex that could correspond to Nurf55 bound to H3/H4 dimers, but also complexes that could correspond to H3/H4 tetramers bound to one Nurf55 (102 kDa) or two Nurf55 (150 kDa) molecules and even higher molecular species (supplemental Fig. S2*B*). In addition, Nurf55 could also bind H3/H4 dimers already bound by other histone chaperones, as has been suggested for Asf1/CIA, which binds histone H3/H4 dimers opposite to the Nurf55 binding site (14).

Interaction of Nurf55 with the PRC2 Component Su(z)12—In the context of PRC2, Nurf55 interacts with Su(z)12 (9, 26). To explore whether this interaction involves the same binding pocket that interacts with the H4 peptide, we coexpressed FLAG-tagged Su(z)12 with wild-type Nurf55 and two Nurf55 mutants (D362A/D365A and L35S/F372S/I373S) that changed the H4 peptide-binding pocket. Wild-type Nurf55 was copurified with FLAG-Su(z)12 in a 1:1 stoichiometry (Fig. 4). In contrast, binding of both Nurf55 mutants to Su(z)12 was dramatically reduced (Fig. 4), indicating that residues involved in H4 peptide binding are also important for binding the PRC2 component Su(z)12. In accordance with the results of Ketel *et al.* (26), we did not observe a direct interaction between Nurf55 and the PRC2 component E(z) (data not shown).

Full-length Su(z)12 protein can be expressed in insect cells but tends to form soluble aggregates when expressed and purified individually. To better characterize the Nurf55-interacting region of Su(z)12, we expressed nine ~100-residue constructs

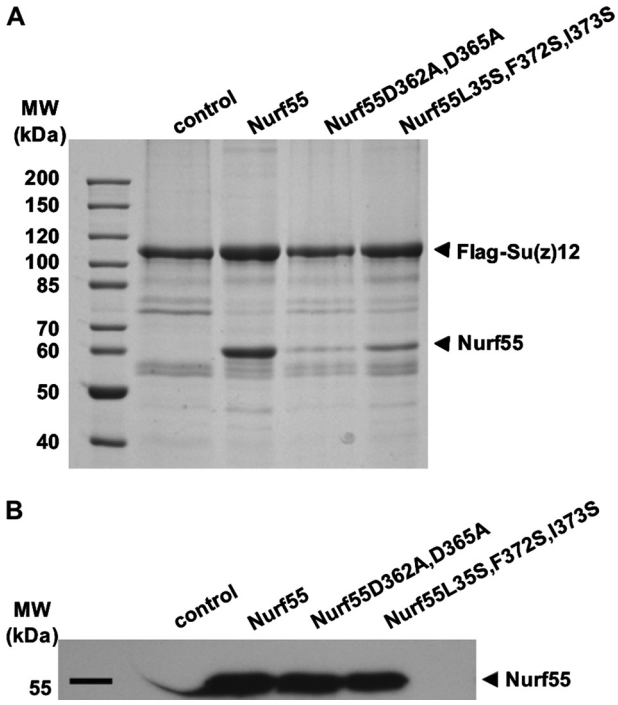

FIGURE 4. **Interaction of Nurf55 with the PRC2 component Su(z)12.** *A*, pulldown experiments of wild-type Nurf55 and mutants D362A/D365A and L35S/F372S/I373S with FLAG-tagged full-length Su(z)12. *B*, Western blot of cell lysates with anti-Nurf55 antibodies demonstrates that wild-type and mutant Nurf55 proteins were expressed at comparable levels.

spanning the entire Su(z)12 protein (Fig. 5*A*). The constructs were chosen to preserve predicted domains and secondary structure elements of Su(z)12 and were expressed in *E. coli* as N-terminal GST fusion proteins (Fig. 5*B*). All constructs were tested for their ability to bind Nurf55 in GST pulldown assays. The N-terminal construct corresponding to the first 100 residues (referred to as Su(z)12-1) showed binding to Nurf55 (Fig. 5*B*, *lower panel*). Using ITC, the Su(z)12-1 construct was found to reproducibly bind Nurf55, although with low affinity (K_D = 24 μM, Table 1). In contrast, no interaction was observed between Su(z)12-1 and two Nurf55 mutants of the H4-binding pocket (D362A/D365A and L35S/F372S/I373S) using ITC and GST pulldown assays (supplemental Fig. S3*A*), consistent with the observation that these mutants did not bind full-length Su(z)12 protein (Fig. 4*A*).

Competition experiments provided additional support for overlapping Nurf55 binding sites for Su(z)12 and histone H4, but not histone H3. In the presence of an excess of the H4

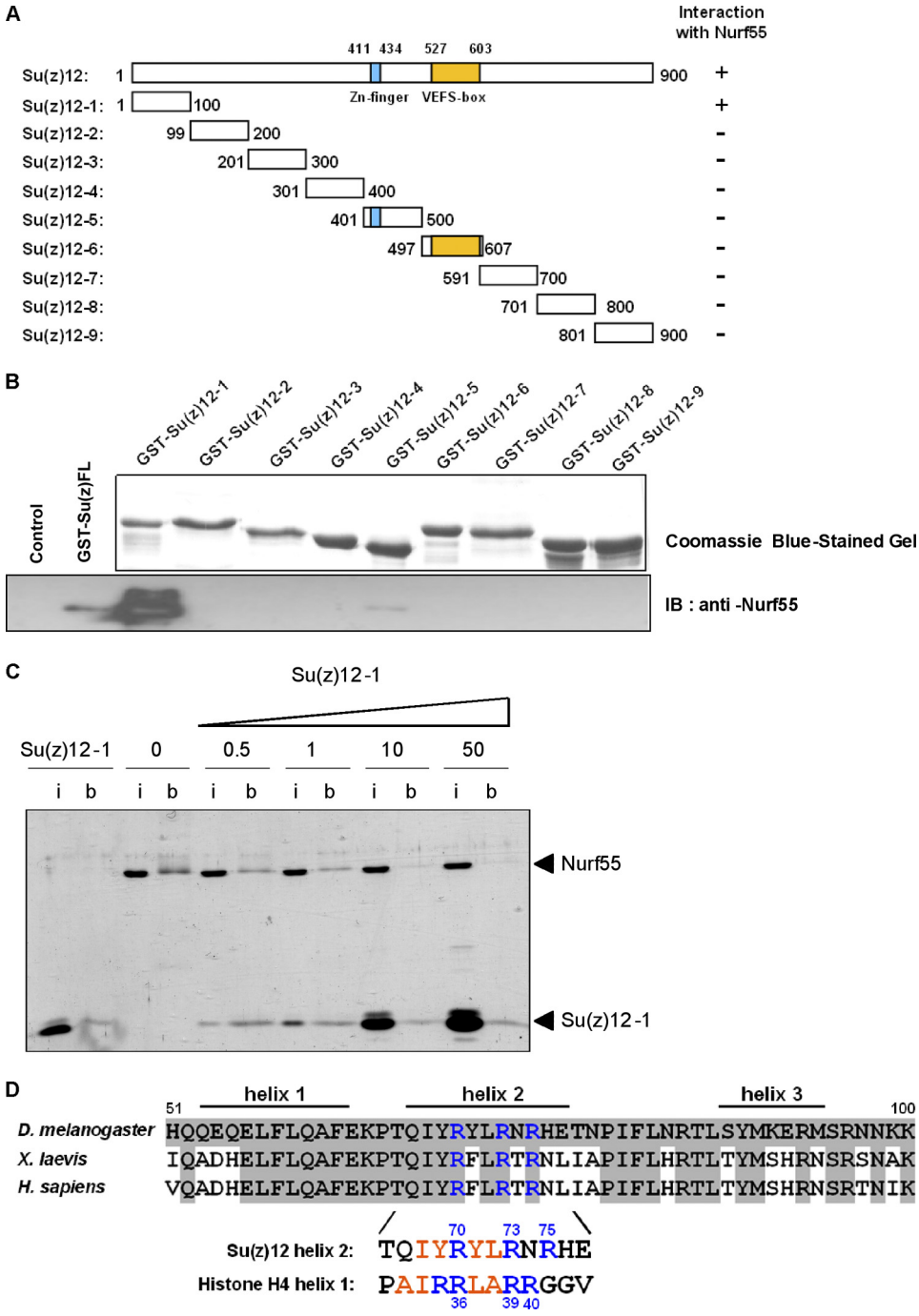

FIGURE 5. **Interaction Nurf55 with the N terminus of Su(z)12.** *A*, full-length Su(z)12 and fragments Su(z)12-1–9 were expressed in *E. coli* as N-terminal GST fusion proteins. Constructs were designed to preserve the predicted zinc finger (residues 411–434), predicted secondary structure elements, and the VEFS homology box (residues 527–603) (27). The results shown in *B* are summarized under *Interaction with Nurf55*. *B*, purification of Su(z)12 fragments using glutathione base affinity purification (*upper panel*) and proteins cleaved from the glutathione beads and analyzed by Western blotting with anti-Nurf55 antibodies (*lower panel*). Only full-length Su(z)12 and the Su(z)12-1 fragment (residues 1–100) bound Nurf55. The low signal of full-length Su(z)12 compared with bacterially expressed Su(z)12-1 presumably results from partial aggregation of this protein. *IB*, immunoblot. *C*, fixed amounts of Nurf55 in the absence or presence of increasing concentrations of Su(z)12-1 (0.5-, 1-, 10-, and 50-fold excess compared with Nurf55 (mol/mol)) were pulled down by peptide $H4_{26-45}$ fixed to Dynabeads. In each experiment, the input lane (*i*) contains one-tenth of the protein used in each of the pulldown assays, and *lane b* corresponds to the bound material. *D*, alignment of residues 51–100 of *Drosophila* Su(z)12 with the corresponding regions in *Xenopus laevis* and human orthologs. Predicted secondary structure elements in Su(z)12 are depicted. Helix 2 of Su(z)12 contains a similar pattern of conserved arginine residues (*blue*) and hydrophobic residues (*red*) as H4 helix 1.

peptide (Table 2), the binding affinity of Nurf55 for Su(z)12-1 was reduced. Consistent with these results, we found that increasing concentrations of Su(z)12-1 abrogated binding of Nurf55 to peptide $H4_{26-45}$ cross-linked to beads in pulldown experiments (Fig. 5*C*). At a 50:1 (mol/mol) ratio of Su(z)12-1 to Nurf55, Nurf55 no longer bound to the H4 peptide. In contrast, an excess of the H3 peptide did not significantly change the binding affinity for Su(z)12-1. In the reverse experiments, an excess of Su(z)12-1 did not change the affinity for the H3 peptide (Table 2).

Although the N-terminal moiety of *Drosophila* Su(z)12 is poorly conserved, the subsequent residues 50–100 of Su(z)12 are predicted to form three α-helices with the second helix (residues 66–80) containing a cluster of arginines (Arg-70, Arg-73, and Arg-75) separated by hydrophobic residues (Fig. 5*D*). This region remarkably resembles H4 helix 1, where three arginines (Arg-36, Arg-39, and Arg-40) also separated by hydrophobic residues play a crucial role in binding to Nurf55. To test whether these arginines of Su(z)12 are involved in binding to Nurf55, they were mutated to alanine, and the mutant Su(z)12-1 protein R70A/R73A/R75A was tested for binding to Nurf55 in a pulldown assay. No binding to Nurf55 was observed (supplemental Fig. S3*B*), suggesting that at least one of the three arginine residues is required for binding. However, a short peptide spanning only residues corresponding to the second predicted helix of Su(z)12 (Su(z)12-1_{63-81}) (Fig. 5*D*) did not bind to Nurf55 in the ITC experiment. Extending this helix toward the N- and C-terminal ends (peptides Su(z)12-1_{45-80} and Su(z)12-1_{63-96}) did not increase the binding affinity, suggesting that an even more extended region of Su(z)12 might be required for Nurf55 binding.

Concluding Remarks—Nurf55 uses a newly identified binding site at the top of the β-propeller for interacting with histone H3 and overlapping binding sites at the propeller edge for binding H4 helix 1 and Su(z)12. In PRC2, Nurf55 and Su(z)12 together provide interaction surfaces to tether the complex to nucleosomes, whereas Nurf55 or Su(z)12 alone is not sufficient for binding (9). Nucleosome binding by PRC2 presumably involves the histone H3-binding site of Nurf55, whereas in the PRC2 complex, histone H4 and Su(z)12 compete for overlapping binding sites. Whether in the PRC2 complex Nurf55 binds only Su(z)12 or both Su(z)12 and histone H4 at different stages of the catalytic process will require further investigation.

Acknowledgments—We thank J. Müller for expression constructs and advice, M. Agez for recombinant histone H3/H4 heterodimers, the Proteomics and the Protein Expression and Purification Core Facilities at EMBL Heidelberg for support, and the European Molecular Biology Laboratory/European Synchrotron Radiation Facility Joint Structural Biology Group for access and support at the European Synchrotron Radiation Facility beamlines.

REFERENCES

1. Simon, J. A., and Kingston, R. E. (2009) *Nat. Rev. Mol. Cell Biol.* **10,** 697–708
2. Schwartz, Y. B., and Pirrotta, V. (2007) *Nat. Rev. Genet.* **8,** 9–22
3. Francis, N. J., Kingston, R. E., and Woodcock, C. L. (2004) *Science* **306,** 1574–1577
4. Czermin, B., Melfi, R., McCabe, D., Seitz, V., Imhof, A., and Pirrotta, V. (2002) *Cell* **111,** 185–196
5. Kuzmichev, A., Nishioka, K., Erdjument-Bromage, H., Tempst, P., and Reinberg, D. (2002) *Genes Dev.* **16,** 2893–2905
6. Müller, J., Hart, C. M., Francis, N. J., Vargas, M. L., Sengupta, A., Wild, B., Miller, E. L., O'Connor, M. B., Kingston, R. E., and Simon, J. A. (2002) *Cell* **111,** 197–208
7. Tie, F., Furuyama, T., Prasad-Sinha, J., Jane, E., and Harte, P. J. (2001) *Development* **128,** 275–286
8. Grimm, C., Matos, R., Ly-Hartig, N., Steuerwald, U., Lindner, D., Rybin, V., Müller, J., and Müller, C. W. (2009) *EMBO J.* **28,** 1965–1977
9. Nekrasov, M., Wild, B., and Müller, J. (2005) *EMBO Rep.* **6,** 348–353
10. Suganuma, T., Pattenden, S. G., and Workman, J. L. (2008) *Genes Dev.* **22,** 1265–1268
11. Furuyama, T., Dalal, Y., and Henikoff, S. (2006) *Proc. Natl. Acad. Sci. U.S.A.* **103,** 6172–6177
12. Tagami, H., Ray-Gallet, D., Almouzni, G., and Nakatani, Y. (2004) *Cell* **116,** 51–61
13. Song, J. J., Garlick, J. D., and Kingston, R. E. (2008) *Genes Dev.* **22,** 1313–1318
14. Murzina, N. V., Pei, X. Y., Zhang, W., Sparkes, M., Vicente-Garcia, J., Pratap, J. V., McLaughlin, S. H., Ben-Shahar, T. R., Verreault, A., Luisi, B. F., and Laue, E. D. (2008) *Structure* **16,** 1077–1085
15. Stirnimann, C. U., Petsalaki, E., Russell, R. B., and Müller, C. W. (2010) *Trends Biochem. Sci.* **35,** 565–574
16. Kabsch, W. (1993) *J. Appl. Crystallogr.* **26,** 795–800
17. McCoy, A. J., Grosse-Kunstleve, R. W., Storoni, L. C., and Read, R. J. (2005) *Acta Crystallogr. D Biol. Crystallogr.* **61,** 458–464
18. Emsley, P., and Cowtan, K. (2004) *Acta Crystallogr. D Biol. Crystallogr.* **60,** 2126–2132
19. Adams, P. D., Grosse-Kunstleve, R. W., Hung, L. W., Ioerger, T. R., McCoy, A. J., Moriarty, N. W., Read, R. J., Sacchettini, J. C., Sauter, N. K., and Terwilliger, T. C. (2002) *Acta Crystallogr. D Biol. Crystallogr.* **58,** 1948–1954
20. Sigurskjold, B. W. (2000) *Anal. Biochem.* **277,** 260–266
21. Tie, F., Stratton, C. A., Kurzhals, R. L., and Harte, P. J. (2007) *Mol. Cell. Biol.* **27,** 2014–2026
22. Verreault, A., Kaufman, P. D., Kobayashi, R., and Stillman, B. (1998) *Curr. Biol.* **8,** 96–108
23. Luger, K., Mäder, A. W., Richmond, R. K., Sargent, D. F., and Richmond, T. J. (1997) *Nature* **389,** 251–260
24. English, C. M., Adkins, M. W., Carson, J. J., Churchill, M. E., and Tyler, J. K. (2006) *Cell* **127,** 495–508
25. Natsume, R., Eitoku, M., Akai, Y., Sano, N., Horikoshi, M., and Senda, T. (2007) *Nature* **446,** 338–341
26. Ketel, C. S., Andersen, E. F., Vargas, M. L., Suh, J., Strome, S., and Simon, J. A. (2005) *Mol. Cell. Biol.* **25,** 6857–6868
27. Finn, R. D., Mistry, J., Tate, J., Coggill, P., Heger, A., Pollington, J. E., Gavin, O. L., Gunasekaran, P., Ceric, G., Forslund, K., Holm, L., Sonnhammer, E. L., Eddy, S. R., and Bateman, A. (2010) *Nucleic Acids Res.* **38,** D211–D222